

Calreticulin Controls the Rate of Assembly of CD1d Molecules in the Endoplasmic Reticulum^{*S}

Received for publication, July 30, 2010, and in revised form, September 15, 2010. Published, JBC Papers in Press, September 22, 2010, DOI 10.1074/jbc.M110.170530

Yajuan Zhu[‡], Wei Zhang[‡], Natacha Veerapen[§], Gurdyal Besra[§], and Peter Cresswell^{†1}

From the [‡]Departments of Immunobiology and Cell Biology, Howard Hughes Medical Institute, Yale University School of Medicine, New Haven, Connecticut 06520-8011 and the [§]Department of Microbial Physiology and Chemistry, School of Biosciences, University of Birmingham, Birmingham B15 2TT, United Kingdom

CD1d is an MHC class I-like molecule comprised of a transmembrane glycoprotein (heavy chain) associated with β_2 -microglobulin (β_2m) that presents lipid antigens to NKT cells. Initial folding of the heavy chain involves its glycan-dependent association with calreticulin (CRT), calnexin (CNX), and the thiol oxidoreductase ERp57, and is followed by assembly with β_2m to form the heterodimer. Here we show that in CRT-deficient cells CD1d heavy chains convert to β_2m -associated dimers at an accelerated rate, indicating faster folding of the heavy chain, while the rate of intracellular transport after assembly is unaffected. Unlike the situation with MHC class I molecules, antigen presentation by CD1d is not impaired in the absence of CRT. Instead, there are elevated levels of stable and functional CD1d on the surface of CRT-deficient cells. Association of the heavy chains with the ER chaperones Grp94 and Bip is observed in the absence of CRT, and these may replace CRT in mediating CD1d folding and assembly. ER retention of free CD1d heavy chains is impaired in CRT-deficient cells, allowing their escape and subsequent expression on the plasma membrane. However, these free heavy chains are rapidly internalized and degraded in lysosomes, indicating that β_2m association is required for the exceptional resistance of CD1d to lysosomal degradation that is normally observed.

CD1 molecules are encoded by a family of linked genes located outside the major histocompatibility complex (MHC)² (reviewed in Ref. 1). In humans, five CD1 isoforms have been identified, including CD1a, b, c, d, and e, that are divided into two groups based on amino acid sequence homology. Group 1 includes CD1a, b, c and e, and group 2 consists only of CD1d. CD1d is the sole CD1 species found in mice and rats. The over-

all structure of CD1 glycoproteins resembles that of MHC class I molecules (2, 3). Each consists of a transmembrane heavy chain that non-covalently associates with β_2m . The heavy chain can be further divided into three extracellular domains ($\alpha 1$, $\alpha 2$ and $\alpha 3$), a transmembrane domain, and a cytoplasmic region. The $\alpha 1$ and $\alpha 2$ domains fold to generate a binding pocket that, unlike MHC class I and class II glycoproteins, which associate with short peptides, binds a lipid. The lipid binding pocket is similar to the peptide binding pocket of MHC molecules, consisting of a pair of antiparallel α -helices overlaying an eight strand β -sheet. CD1 binding pockets are deep and highly hydrophobic, and can accommodate the alkyl chains of a wide variety of lipids (4). Similar to the way that MHC class I- and class II-restricted T cells can recognize peptide antigens presented by MHC glycoproteins, lipid antigens associated with CD1 molecules can also be recognized by effector T cells (5, 6). In particular, CD1d molecules present lipids to a unique subpopulation of T lymphocytes, called NKT cells, which co-express an invariant T cell receptor (TCR) and surface markers also found on natural killer (NK) cells (7). Recent data have shown that both endogenous lipids and exogenous lipids, *e.g.* from *Sphingomonas* and *Borrelia burgdorferi* species, can be presented to NKT cells by CD1d molecules (8–12). Upon activation, NKT cells secrete both T helper type 1 and type 2 cytokines, and play important roles in both innate and adaptive immunity (13).

The presentation of lipid antigens depends on the proper assembly and intracellular trafficking of CD1 glycoproteins. Shortly after their synthesis in the endoplasmic reticulum (ER) and assembly with β_2m , CD1d molecules follow the secretory pathway to the cell surface (14, 15). From there, CD1d is routed to endosomal compartments by a tyrosine-based motif, YXXZ (where Y is tyrosine, X is any amino acid, and Z is a bulky hydrophobic amino acid), located in its cytoplasmic domain (16). Adaptor proteins (AP) bind to this motif at the plasma membrane and direct the internalization of CD1d molecules via clathrin-coated pits (17, 18). Binding of lipid antigens to CD1d molecules occurs mainly in the endocytic system and is catalyzed by endosomal lipid transfer proteins, predominantly the saposins (19–21). Abolishing endosomal targeting of CD1d, by mutating the endocytic motif, or disrupting lysosomal acidification, which affects saposin function, significantly impairs antigen presentation by CD1d (22, 23). In addition to accessing the endocytic pathway by AP-dependent endocytosis, CD1d molecules can also be directed there through an interaction with the invari-

* This work was supported, in whole or in part, by National Institutes of Health Grant R01 AI059167 (to P. C.) and the Howard Hughes Medical Institute.
[‡] Author's Choice—Final version full access.

^S The on-line version of this article (available at <http://www.jbc.org>) contains supplemental Figs. S1 and S2.

¹ To whom correspondence should be addressed: Yale University School of Medicine, Dept. of Immunobiology, 300 Cedar St., PO Box 208011, New Haven, CT 06520-8011. Tel.: 203-785-5176; Fax: 203-785-4461; E-mail: peter.cresswell@yale.edu.

² The abbreviations used are: MHC, major histocompatibility complex; Bip, immunoglobulin-binding protein; CD1, cluster of differentiation 1; β_2m , β_2 -microglobulin; ER, endoplasmic reticulum; CNX, calnexin; CRT, calreticulin; α -GalCer, α -galactosyl ceramide; CST, castanospermine; GalGalCer, galactosyl-b(b1–2)-galactosyl ceramide; NKT, natural killer T cells; Endo H, endoglycosidase H; AP, adaptor protein; DSP, dithiobis succinimidylo propionate; CHX, cycloheximide.

Role of Calreticulin in CD1d Assembly

ant chain, normally responsible for the endocytic localization of MHC class II molecules, or by an association with MHC class II-invariant chain complexes (16, 24). The functional significance of this alternative route for endosomal assessment is unclear. Nevertheless, there is evidence that CD1d molecules can undergo multiple rounds of recycling between the cell surface and endosomal compartments to extensively survey changes in lipid composition (16, 22). Associated lipid antigens are presented at the plasma membrane for NKT cell recognition.

Previous studies have identified accessory molecules involved in the early biogenesis of CD1d molecules inside the ER (14, 15, 25). Like other glycoproteins, the correct folding of CD1d involves the lectin chaperones (15). After translocation into the ER, newly synthesized CD1d heavy chains are rapidly glycosylated and bind calreticulin (CRT) and calnexin (CNX), which recognize monoglucosylated *N*-linked glycans. These ER chaperones recruit the thiol oxidoreductase ERp57, which catalyzes disulfide bond formation in CD1d heavy chains. Once released from the CNX/CRT cycle, fully oxidized CD1d heavy chains associate with β_2m and enter the Golgi where the glycans are further processed before transport to the plasma membrane. Unlike MHC class I and CD1b molecules, association with β_2m is not strictly required for CD1d to exit the ER and small amounts of free CD1d heavy chains expressed on the cell surface may still be functional (26–29). Consistent with the hypothesis that CD1 molecules are loaded with endogenous lipids during assembly inside the ER, multiple groups have found the association of ER-derived lipids with ER-retained or -secreted soluble CD1d (30–32). Loading of ER-derived lipids to nascent CD1d molecules may be mediated by microsomal triglyceride transfer protein (MTP), the only known lipid transfer protein found in the ER (33, 34). However the role of lipids in the quality control of CD1d assembly is poorly understood.

The assembly of MHC class I molecules also requires lectin chaperones, including CRT. The role of CRT in MHC class I antigen presentation has been studied in CRT-deficient murine embryonic fibroblasts (MEFs) (35, 36). In such cells, MHC class I molecules assemble with β_2m normally and move to the cell surface with accelerated kinetics. However, loading with optimal peptides within the peptide loading complex inside the ER is defective. Consequently a large fraction of MHC class I associates with low-affinity peptides and is unstable, and T cell recognition is impaired. These results demonstrated a key role for CRT in the quality control of class I-peptide complexes, and inspired us to examine the role of CRT in the assembly and function of CD1d molecules.

In this study, we have examined the assembly and antigen presentation functions of CD1d in CRT-deficient MEFs. We find that neither of these functions is impaired. Instead, we observed accelerated conversion of CD1d free heavy chains to β_2m -associated dimers and the accumulation of elevated levels of stable and functional dimers on the cell surface. However, ER retention of free CD1d heavy chains is not efficient in the absence of CRT, resulting in the expression of free heavy chains on the plasma membrane.

EXPERIMENTAL PROCEDURES

Cell Lines and Stable Transfectants—Wild-type (K41) and CRT-deficient (K42) fibroblasts were gifts from Dr. David Williams, University of Toronto. The fibroblasts and their transfectants were maintained in Iscove's modified Dulbecco's medium (Sigma) supplemented with 10% fetal bovine serum (Hyclone) at 37 °C in 5% CO₂ atmosphere. The mouse V α 14J α 18 invariant TCR-positive cell hybridoma, DN32.D3, was kindly provided by Dr. Albert Bendelac, University of Chicago.

The RetroMax Retroviral System (Imgenex) was used to express CD1d in K41 and K42 cells. Briefly, human CD1d cDNA was subcloned into the MSCV2.2 IRES-GFP vector to generate a CD1d-IRES-GFP construct. The vector was co-transfected into the packaging cell line 293T with pCL-Eco packing vector. 24–48 h after transfection the virus supernatant was harvested to infect K41 and K42 cells and stable transfectants were sorted by flow cytometry using GFP expression. The pQCXIH vector containing wild-type mouse CRT cDNA was provided by Dr. D. Williams and was transduced into K42.CD1d cells as described (37).

Antibodies and Reagents—The monoclonal mouse antibodies (mAbs) to human CD1d, CD1d51, and D5, have been previously described (15). The polyclonal rabbit anti-CRT antibody, the rat anti-Grp94 mAb, and the polyclonal rabbit anti-Bip (Grp78) antibody were from Stressgen. The mouse anti-GAPDH mAb was from RDI. The mouse anti-GFP mAb was from Clontech. The rat anti-Lamp1 mAb was from the Developmental Studies Hybridoma Bank. The glycosidases Endo H and PNGase F were from New England Biolabs. Brefeldin A and cycloheximide were from Sigma-Aldrich. α -GalCer and galactosyl-(α 1–2)-galactosyl ceramide (GalGalCer) were synthesized as described (38).

Western Blotting—Western blot analyses were performed as previously described (25). For quantitative Western blots, the protein content of the post-nuclear supernatant was quantified by Bradford assay (BioRad) and 3-fold serial dilutions were resolved by SDS-PAGE. Following primary antibody incubation, membranes were probed with alkaline phosphatase-coupled secondary antibody (1:5000) (Jackson Labs) and imaged using a fluorimager with ECF substrate (Amersham Biosciences).

Metabolic Labeling and Immunoprecipitation—MEF transfectants were harvested, washed, starved for 1 h in medium without methionine/cysteine, pulse-labeled with ³⁵S labeling mix (PerkinElmer Life Sciences), chased in an excess of unlabeled methionine/cysteine for the indicated times and washed with cold PBS. For experiments examining the lectin-mediated retention of CD1d within the ER, cells were starved and labeled without castanospermine (CST) (Sigma) and chased in the presence of 2 mM CST as indicated.

For all immunoprecipitation experiments except as otherwise indicated, cells were solubilized in 1% digitonin in TBS with a proteinase inhibitor mixture (Roche). Post-nuclear supernatants were precleared with normal rabbit or mouse serum and protein G-Sepharose (GE healthcare) prior to specific immunoprecipitation with the indicated antibody and

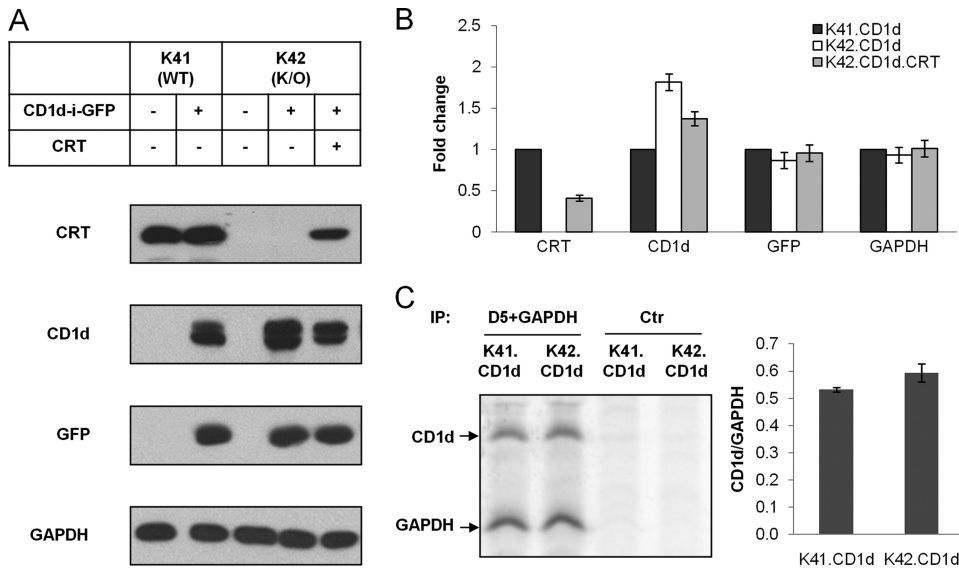


FIGURE 1. Elevated steady state CD1d protein levels in the absence of CRT. *A*, the expression of CRT, CD1d, GFP and GAPDH was examined by Western blot in K41 cells, K41 transduced with CD1d-IRES-GFP (*CD1d-i-GFP*), K42 cells, K42 transduced with CD1d-IRES-GFP, and K42 transduced with CD1d-IRES-GFP and CRT. *B*, the expression of CRT, CD1d, GFP, and GAPDH in K41.CD1d, K42.CD1d and K42.CD1d.CRT cells was assessed by quantitative Western blot. The level of each protein in K42.CD1d or K42.CD1d.CRT cells was calculated as fold change relative to that in K41.CD1d cells. Data shown are the average \pm S.E. of three dilutions from two separate experiments. *C*, initial CD1d protein synthesis rates in K41.CD1d and K42.CD1d cells were assessed by a short metabolic labeling experiment. Cells were labeled with [35 S]methionine/cysteine for 5 min and extracted in 1% digitonin. The extracts were then immunoprecipitated by D5 (anti-CD1d free heavy chain) together with GAPDH antibody, as the internal control, or by a nonrelated control antibody (*Ctrl*). The immunoprecipitates were eluted by boiling in the reducing SDS-sample buffer and analyzed by 10% SDS-PAGE (*left panel*). *Right panel*, quantification of band intensities using Bio-Rad GS-525 phosphorimaging: D5 over GAPDH signal. Data shown are the average \pm S.E. of three independent experiments.

protein G-Sepharose. For re-precipitation, immunoprecipitated proteins were eluted by heating to 95 °C in 1% SDS, 5 mM dithiothreitol. The eluted material was then diluted into 1% Triton X-100 in TBS and free CD1d heavy chains precipitated with D5 mAb and protein G-Sepharose prior to SDS-PAGE. When Endo H digestion was performed, precipitated proteins were eluted using Endo H buffer, and incubated overnight with Endo H, as suggested by the manufacturer.

Flow Cytometric Analysis—Cells (0.5×10^6) were stained as previously described (25) and analyzed using a Becton Dickinson FACScalibur (Mountain View, CA).

NKT Cell Stimulation Assay—MEF cells transfected with CD1d were incubated with α -GalCer for 4 h or GalGalCer overnight. After three washes in PBS, the cells were fixed in 0.05% glutaraldehyde for 30 s, quenched with an equal volume of 0.4 M glycine and washed in medium three times. The fixed cells (1×10^5 cells/well) were then plated in triplicate in 96-well plates and co-cultured with 1×10^5 DN32.D3 cells/well for 24 h. Secreted mIL-2 was detected by an Opti-ELISA kit from BD Pharmingen following the manufacturer's instructions.

Cross-linking—Cells were lysed on ice in bicine buffer (0.13 M NaCl, 0.02 M Bicine, pH 8.2) containing 1% Triton X-100, 200 μ g/ml dithiobis (succinimidylyl propionate) (DSP) (Thermo Scientific), and the proteinase inhibitor mixture. Lysates were quenched with 10 mM glycine before immunoprecipitation.

Confocal Immunofluorescence—Cells growing on cover slips were fixed at room temperature for 15 min in 3% formaldehyde, quenched with 10 mM glycine for 10 min and permeabilized

in PBS containing 0.5% saponin (Sigma-Aldrich) and 0.5% BSA. For co-staining, cells were incubated with D5 mouse mAb and rat anti-Lamp1 mAb, followed by Alexa Fluor 546-conjugated highly cross-absorbed goat anti-mouse IgG and Alexa Fluor 633-conjugated goat anti-rat IgG antibodies (Molecular Probes). All images were acquired by using a Leica TCS SP2 confocal system and processed with Leica software.

RESULTS

Higher Steady State Levels and Lower ER Retention of CD1d in the Absence of CRT—To investigate the role of CRT in the assembly of CD1d molecules, we used the CRT-sufficient MEF cell line K41 and its CRT-deficient counterpart K42. Because MEF cells have no detectable CD1d expression (20), we retrovirally transduced a CD1d-IRES-GFP construct into K41 and K42 cells to generate the stable transfectants K41.CD1d and K42.CD1d. The internal ribosome entry site (IRES) from encephalomyocarditis

virus (ECMV) between the CD1d- and GFP-coding regions permitted both genes to be translated from a single bicistronic mRNA. We used flow cytometry to sort stably transduced cell populations that expressed similar levels of GFP, assessed by Western blotting (Fig. 1, *A* and *B*) or flow cytometry (Fig. 4*A*). As expected, this resulted in equal rates of CD1d protein synthesis in both transfected cell lines as determined by a short metabolic labeling experiment (Fig. 1*C*). However, when steady state protein levels were assessed by Western blot, CD1d levels were found to be substantially higher in the absence of CRT (Fig. 1*A*, compare *lanes 2* and *4*, and Fig. 1*B*). Quantitative Western blotting showed that steady state protein levels of CD1d in CRT-deficient K42.CD1d cells are \sim 2-fold higher than in CRT-sufficient K41.CD1d cells. In contrast, levels of GFP and GAPDH, two non-glycoproteins, were indistinguishable in the two cell lines (Fig. 1, *A* and *B*). To confirm that the elevated CD1d level was caused by the absence of CRT, we reconstituted CRT expression in K42.CD1d, generating the cell line K42.CD1d.CRT. Introduction of CRT caused a significant decrease in CD1d steady state protein levels (Fig. 1*A*, compare *lanes 4* and *5* and Fig. 1*B*), whereas levels of GFP and GAPDH remained unaffected. The CD1d level in K42.CD1d.CRT still remained somewhat above that in K41.CD1d, which may be because of the \sim 2-fold higher CRT expression in the latter (Fig. 1*A*, compare *lanes 2* and *5* and Fig. 1*B*).

CD1d ran as a doublet upon SDS-PAGE (Figs. 1*A* and 2*A*), and we speculated that the two bands correspond to different glycosylation isoforms. Consistent with this, treatment of

Role of Calreticulin in CD1d Assembly

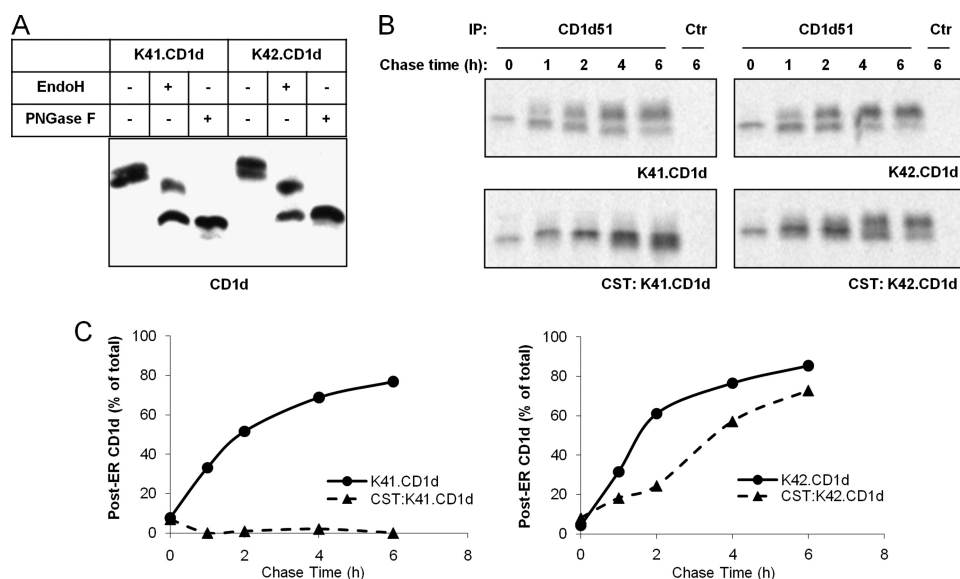


FIGURE 2. Inefficient ER retention in the absence of CRT. *A*, the glycosylation patterns of the steady state CD1d molecules in K41.CD1d and K42.CD1d cells were examined by Endo H or PNGase F digestion. Whole cell lysates were denatured by boiling in 0.5% SDS and 40 mM DTT for 10 min and incubated with Endo H or PNGase F or mock treated overnight. The samples were then resolved by SDS-PAGE and blotted with D5 antibody. *B* and *C*, CST treatment blocked the ER exit of CD1d/ β_2 m dimers in K41.CD1d, but not K42.CD1d cells. *B*, K41.CD1d and K42.CD1d cells were labeled with [35 S]methionine/cysteine in the absence of CST for 15 min and chased with or without 2.5 mM CST for up to 6 h. Cells were lysed in 1% digitonin, immunoprecipitated with CD1d51 (anti-CD1d/ β_2 m) or a control antibody (Ctr). SDS-stripped proteins were re-immunoprecipitated with D5, treated with Endo H, and analyzed by SDS-PAGE. *C*, quantification of the results in panel *B*. Post-ER CD1d was calculated as the percentage of total CD1d that was Endo H-resistant. The data shown represent one of two independent experiments.

whole cell lysates with peptide-*N*-glycosidase F (PNGase F), which cleaves *N*-linked oligosaccharides from glycoproteins, gave rise to a single CD1d band with a substantially lower apparent molecular weight (Fig. 2*A*). CD1d has four *N*-linked glycosylation sites, one of which, at position Asn-42, fails to be processed to the complex form in the Golgi apparatus because of its proximity to the associated β_2 m (25) and remains sensitive to the enzyme endoglycosidase H (Endo H). When detergent lysates were treated with Endo H, subjected to SDS-PAGE and blotted for CD1d, two major bands were observed, which represent the partially Endo H-resistant post-ER CD1d and the Endo H-sensitive ER-localized CD1d (Fig. 2*A*). In K41.CD1d cells the Endo H-sensitive ER form of CD1d was present at a substantially higher level, whereas K42.CD1d cells contained more partially Endo H-resistant post-ER forms (Fig. 2*A*, compare lanes 2 and 5). The data indicate that in the absence of CRT ER retention of CD1d is lower despite the higher steady state level.

We previously observed that the interaction of CD1d free heavy chains with CRT and CNX is glycosylation-dependent (15). After the core Glc₃Man₉GlcNAc₂ oligosaccharide is transferred onto newly synthesized CD1d free heavy chains, it is trimmed by glucosidases I and II to the Glc₁Man₉GlcNAc₂ processing intermediate, which is the specific ligand for CRT and CNX (39, 40). If the generation of this monoglucosylated folding intermediate is inhibited by the glucosidase inhibitor CST, CRT and CNX fail to interact with CD1d (15). Moreover, as for other glycoprotein substrates (41, 42), dissociation of CRT and CNX from CD1d heavy chains is dependent on trimming of the terminal glucose from the glycan (15). The observed

increase in Endo H-sensitive CD1d when CRT is present suggested that CRT might be a critical retention factor. To examine this question, K41.CD1d and K42.CD1d cells were pulse-labeled with [35 S]methionine/cysteine without CST for 15 min and chased in the presence of CST for various times to inhibit the removal of the terminal glucose. CD1d remained completely sensitive to Endo H in CST-treated CRT-sufficient K41.CD1d cells (Fig. 2, *B*, left panels and *C*, left panel), indicating a block in release from the ER. However, although the rate of transport was reduced in CRT-deficient K42.CD1d cells upon CST treatment the block was far from incomplete (Fig. 2, *B*, right panel and *C*, right panel). Because CNX is the only remaining lectin chaperone in K42.CD1d cells, these results strongly suggest that CRT is superior to CNX in retaining CD1d inside the ER.

CD1d Assembly Is Accelerated in the Absence of CRT—To examine

the assembly and maturation kinetics of CD1d in the presence and absence of CRT, K41.CD1d and K42.CD1d cells were labeled with [35 S]methionine/cysteine for 15 min and chased up to 6 h. Cells were lysed in 1% digitonin, a condition where CD1d association with β_2 m is best maintained (15), and immunoprecipitates generated from the lysates using the anti-CD1d antibodies D5 and CD1d51, which recognize free heavy chains and heavy chain- β_2 m dimers, respectively (15, 43). Exit from the ER was monitored by loss of susceptibility to Endo H. Consistent with previous results (15, 25), Endo H-sensitive free heavy chains gradually converted to β_2 m-associated dimers (Fig. 3*A*). Once converted to dimers, CD1d rapidly trafficked through the Golgi, indicated by the acquisition of Endo H-resistance. Formation of CD1d/ β_2 m dimers proceeded more rapidly in CRT-deficient K42.CD1d cells than in CRT-sufficient K41.CD1d cells. At the beginning of the chase (0 h), less than 5% of total CD1d had converted to CD1d/ β_2 m complex in K41.CD1d cells, and it took about 4 h to achieve 50% dimer formation (Fig. 3*B*, left panel). In sharp contrast, more than 10% of total CD1d already existed as dimers at the beginning of the chase in K42.CD1d cells and dimer formation reached 50% in less than two hours (Fig. 3*B*, left panel). In addition, when CRT was re-expressed in K42.CD1d cells, dimer formation was significantly slowed, indicating that CD1d/ β_2 m assembly was reduced. Once CD1d- β_2 m dimerization occurred, however, the dimers trafficked out of the ER at comparable rates in all three cell lines, determined by the acquisition of Endo H-resistance (Fig. 3*B*, right panel). Hence, CRT appears to

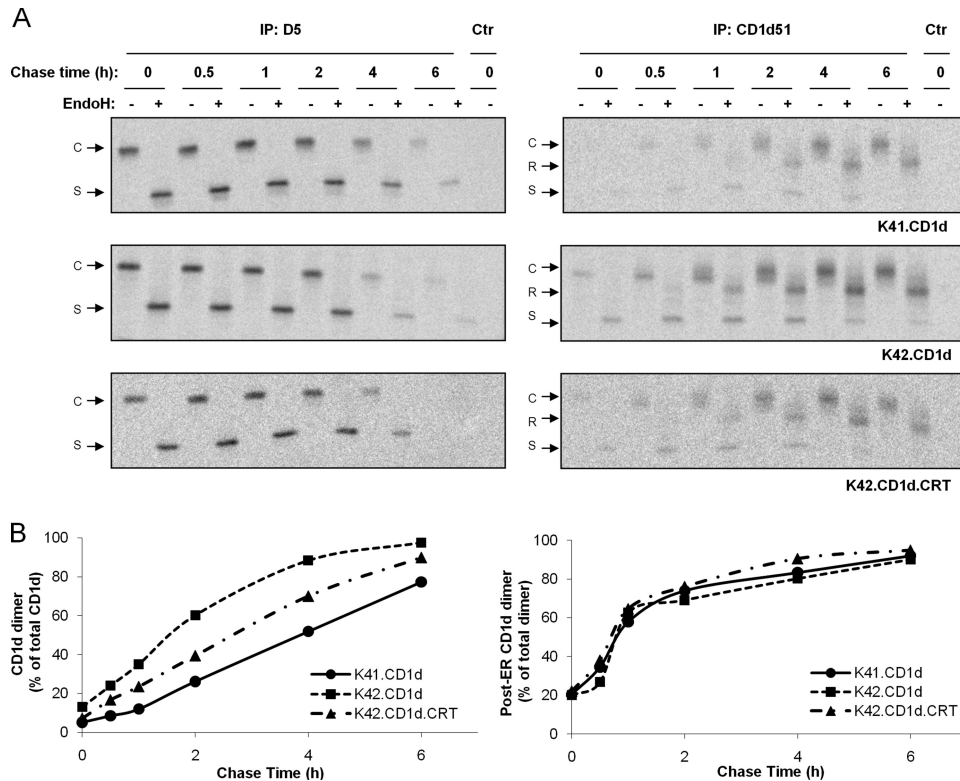


FIGURE 3. Accelerated CD1d assembly in the absence of CRT. *A*, the maturation kinetics of newly synthesized CD1d proteins was analyzed by pulse-chase experiments. K41.CD1d, K42.CD1d or K42.CD1d.CRT cells were labeled with [³⁵S]methionine/cysteine for 15 min and chased for up to 6 h. The cells were extracted at the times shown in 1% digitonin and immunoprecipitated with CD1d51 (anti-CD1d/β₂m), D5 (anti-CD1d free heavy chain) or a control antibody (Ctr). Stripped proteins were re-immunoprecipitated with D5 and immunoprecipitates were eluted, incubated with or without Endo H overnight before analysis by SDS-PAGE. Different forms of CD1d bands are indicated: C, control with no Endo H treatment; R, Endo H-resistant; S, Endo H-sensitive. *B*, quantification of data in *panel A*; *Left panel*, conversion of CD1d free heavy chains to β₂m-associated dimers as calculated by their percentage of total CD1d. *Right panel*, the percentage of post-ER forms of CD1d as calculated by fraction that is Endo H-resistant. The data represent one of at least three independent experiments.

affect the rate of dimer formation but not transport after assembly.

Surface CD1d Levels Are Elevated in the Absence of CRT—MHC class I molecules assembled in CRT-negative cells contained peptide ligands of lower affinity, and were less stable than those in wild-type cells, but were nevertheless transported more rapidly to the cell surface (35, 36). Consequently, reduced surface MHC class I expression and impaired MHC class I-mediated antigen presentation were observed in K42 cells when compared with their CRT-sufficient counterpart K41 (35). In contrast, although CD1d molecules assemble faster in the absence of CRT, they clearly retain stability, because substantially more CD1d protein accumulates at steady state in K42.CD1d (Fig. 1). Consistent with this, we observed elevated levels of surface CD1d in the absence of CRT (Fig. 4*A*, *right histograms and bar diagram*), while the co-expressed GFP levels were unaffected (Fig. 4*A*, *left histograms and bar diagram*). Surface CD1d levels on K42.CD1d cells were ~1.7-fold higher than on K41.CD1d cells. Moreover, restoration of CRT expression in K42.CD1d.CRT cells decreased surface expression, while GFP-expression remained unaffected.

To examine whether CD1d molecules assembled in the absence of CRT are functional, we studied the CD1d-mediated presentation of α-galactosylceramide (α-GalCer)

and galactosyl-(α1-2)-galactosylceramide (GalGalCer) to the CD1d-restricted T cell hybridoma DN32.D3 which expresses the canonical NKT cell Vα14-Jα18 T cell receptor (7, 44). CD1d-associated α-GalCer is a potent stimulator of all Vα14-Jα18 T cell receptor-expressing murine NKT cells and human NKT cells expressing the Vα24-Jα18 T cell receptor (45, 46). α-GalCer can be loaded onto cellular CD1d by direct exchange at the plasma membrane or in the endocytic system (20, 47), whereas its derivative GalGalCer can bind to CD1d, but cannot stimulate NKT cells unless the terminal galactose residue is removed by lysosomal α-galactosidase to generate α-GalCer (48). The CD1d-transfected CRT-positive or negative cell lines were incubated with different concentrations of α-GalCer or GalGalCer, and subsequently washed and fixed before co-culturing them with DN32.D3 cells. The culture supernatants were assayed for secreted IL-2 by a sandwich ELISA. Fig. 4*B* shows that the presentation of α-GalCer and GalGalCer was not impaired by the absence of CRT. In fact, the activation of NKT cells by

lipid-loaded K42.CD1d cells was substantially higher than that observed for their CRT-sufficient counterpart K41.CD1d. This likely reflects the higher surface-CD1d levels (Fig. 4*A*). In keeping with this, the re-expression of CRT in K42.CD1d.CRT cells not only decreased both total (Fig. 1, *A* and *B*) and surface (Fig. 4*A*) CD1d levels, but also substantially reduced NKT cell activation (Fig. 4*B*).

The accumulation of functional CD1d on the cell surface suggests that unlike MHC class I, CD1d molecules assembled in the absence of CRT are stable. To further corroborate this, we examined the stability of CD1d/β₂m dimers assembled in the absence or presence of CRT. Different detergents have variable effects on protein-protein interactions and we previously developed an assay to discriminate between stable and unstable CD1d/β₂m dimers in different detergents (25). Using the same method we observed that CD1d/β₂m dimers assembled in K41.CD1d and K42.CD1d cells had similar stabilities in digitonin and Triton X-100 (*supplemental Fig. S1A*). We additionally analyzed the thermostability of CD1d/β₂m dimers (*supplemental Fig. S1B*) and their stability under acidic conditions (*supplemental Fig. S1C*), adapting assays that have been used by others to examine the stability of MHC class I/β₂m complexes (49, 50). Similar to MHC class I molecules, CD1d/β₂m dimers were progressively disrupted with increasing temperature or

Role of Calreticulin in CD1d Assembly

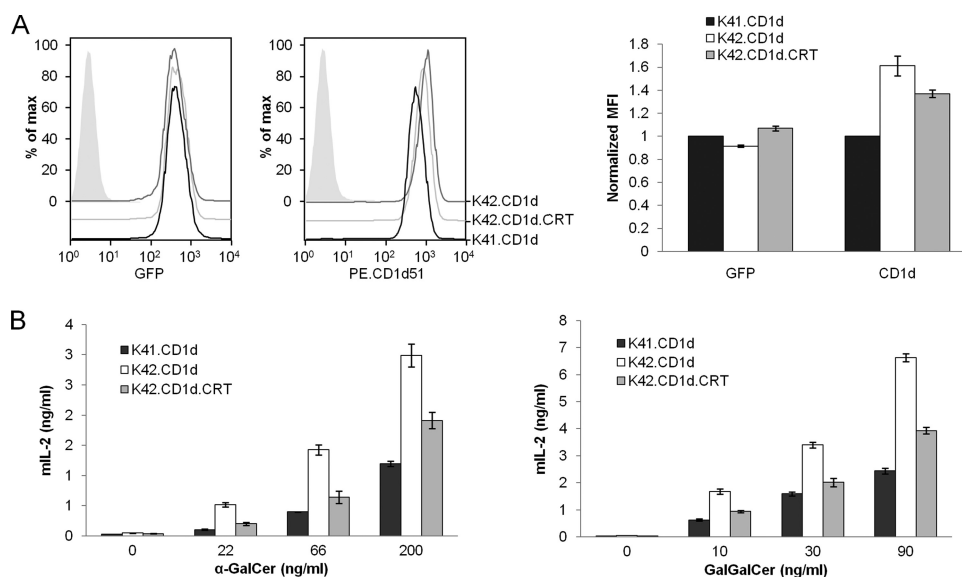


FIGURE 4. Absence of CRT promotes elevated levels of functional surface CD1d. *A*, surface expression of β_2m -associated CD1d dimers on K41.CD1d, K42.CD1d and K42.CD1d.CRT cells was examined by flow cytometry using the CD1d51 antibody (unfilled histograms, *middle panel*). Corresponding GFP expression in each cell type was also assessed by flow cytometry (unfilled histograms, *left panel*). Background staining was analyzed by incubating parental CD1d-negative MEFs with CD1d51 antibody (filled histograms, *left and middle panels*). *Right panel*, statistical analysis of the data in *left and middle panels*. MFI values of K42.CD1d and K42.CD1d.CRT were normalized against that of K41.CD1d cells. Data shown are the average \pm S.E. of three separate experiments. *B*, presentation of α -GalCer and GalGalCer by K41.CD1d, K42.CD1d and K42.CD1d.CRT. Cells were incubated with different concentrations of α -GalCer for 4 h (*left panel*) or with GalGalCer overnight (*right panel*). After washing and fixing, the cells were co-cultured with the mouse NKT hybridoma, DN32.D3, in triplicate. Secretion of mIL-2 into the medium was analyzed after 24 h by sandwich ELISA. Results were expressed as the mean \pm S.E. of triplicate values. The data shown represent one of two independent experiments.

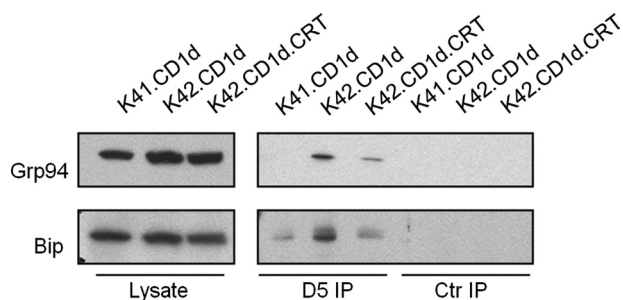


FIGURE 5. Absence of CRT correlates with enhanced interaction of CD1d with Grp94 and Bip. K41.CD1d, K42.CD1d and K42.CD1d.CRT cells were extracted in 1% TritonX-100 in Bicine buffer, pH 8.0, in the presence of 200 μ g/ml DSP. Residual DSP was quenched using 10 mM glycine, and the extracts were precipitated with D5 (anti-CD1d free heavy chain, *D5 IP*) or a control antibody (*Ctr IP*). Immunoprecipitates were separated by SDS-PAGE and Western blots probed for Grp94 and Bip. The relative amounts of Grp94 and Bip in these cell lines were evaluated by directly immunoblotting the cell lysate (*Lysate*).

lower pH. However, we did not observe substantial differences in their stability when assembled in K41.CD1d or K42.CD1d cells in either assay (*supplemental Fig. S1, B and C*). Thus, unlike MHC class I molecules, CD1d/ β_2m dimers assembled in the absence of CRT appear to be fully stable and functional.

CD1d Interactions with Grp94 and Bip Are Enhanced in the Absence of CRT—The normal function and stability of CD1d in K42.CD1d cells suggested that other chaperones might facilitate CD1d folding in the absence of CRT. To address this possibility, we used co-immunoprecipitation to assess potential interactions between CD1d and other chaperones. Because detergents disrupt the association of some chaperones with substrates, we used the reducible cross-linking reagent DSP to

preserve such interactions. After MEF cell lines were lysed in 1% Triton X-100 in the presence of 200 μ g/ml DSP, the extracts were immunoprecipitated with D5 antibodies to recover free CD1d heavy chains and associated proteins. A human MHC class I antibody was used as a negative control. Immunoprecipitated material was resolved by reducing SDS-PAGE, and associated chaperones were detected by Western blot. Consistent with previous results (15), no association of Grp94 with CD1d was detected in wild-type cells (*Fig. 5*). In CRT-deficient cells, however, Grp94 was associated with free CD1d heavy chains, and the level of associated Grp94 was reduced after re-expression of CRT in K42.CD1d.CRT cells. Moreover, we detected a weak association of Bip with free CD1d heavy chains in K41.CD1d cells, while the levels of associated Bip increased significantly in K42.CD1d cells (*Fig. 5*). Again, re-expression of CRT in K42.CD1d.CRT cells resulted in

reduced Bip association of CD1d. No Grp94 or Bip was recovered by the control antibody. Thus Grp94 and Bip may replace the function of CRT in facilitating CD1d folding in K42.CD1d cells.

Free CD1d Heavy Chains Can Escape the ER in the Absence of CRT—We and other investigators (15, 43) have shown that the majority of free CD1d heavy chains convert to CD1d/ β_2m dimers before exit from the ER. Consequently, CD1d molecules expressed on the cell surface are predominantly β_2m -associated. Consistent with this model, we observed high levels of CD1d/ β_2m dimers on the surface of K41.CD1d and K42.CD1d cells by flow cytometry (*Fig. 4A*). However, significant expression of free CD1d heavy chains was also detected on the surface of the CRT-deficient cells (*Fig. 6A*). Surface free heavy chain expression on K42.CD1d cells was about 3-fold higher than on K41.CD1d cells, and re-expression of CRT led to a substantial reduction (*Fig. 6A, right panel*). The presence of free CD1d heavy chains on the cell surface in the absence of CRT was also confirmed using immunoprecipitation. To capture only surface-exposed CD1d molecules, live K41 and K42 derivatives were incubated on ice for 30 min with D5, CD1d51 or a control antibody, respectively. After washing, the cells were lysed in 1% digitonin and protein G-Sepharose was added to isolate surface proteins associated with these antibodies. Eluted immunoprecipitates were treated with Endo H overnight before they were resolved by SDS-PAGE and blotted using a biotin-labeled D5 antibody. For comparison, the total CD1d proteins in K41.CD1d and K42.CD1d cells were also captured from detergent lysates by the addition of antibodies and protein G-Sepharose. As expected, the data showed that the majority of CD1d

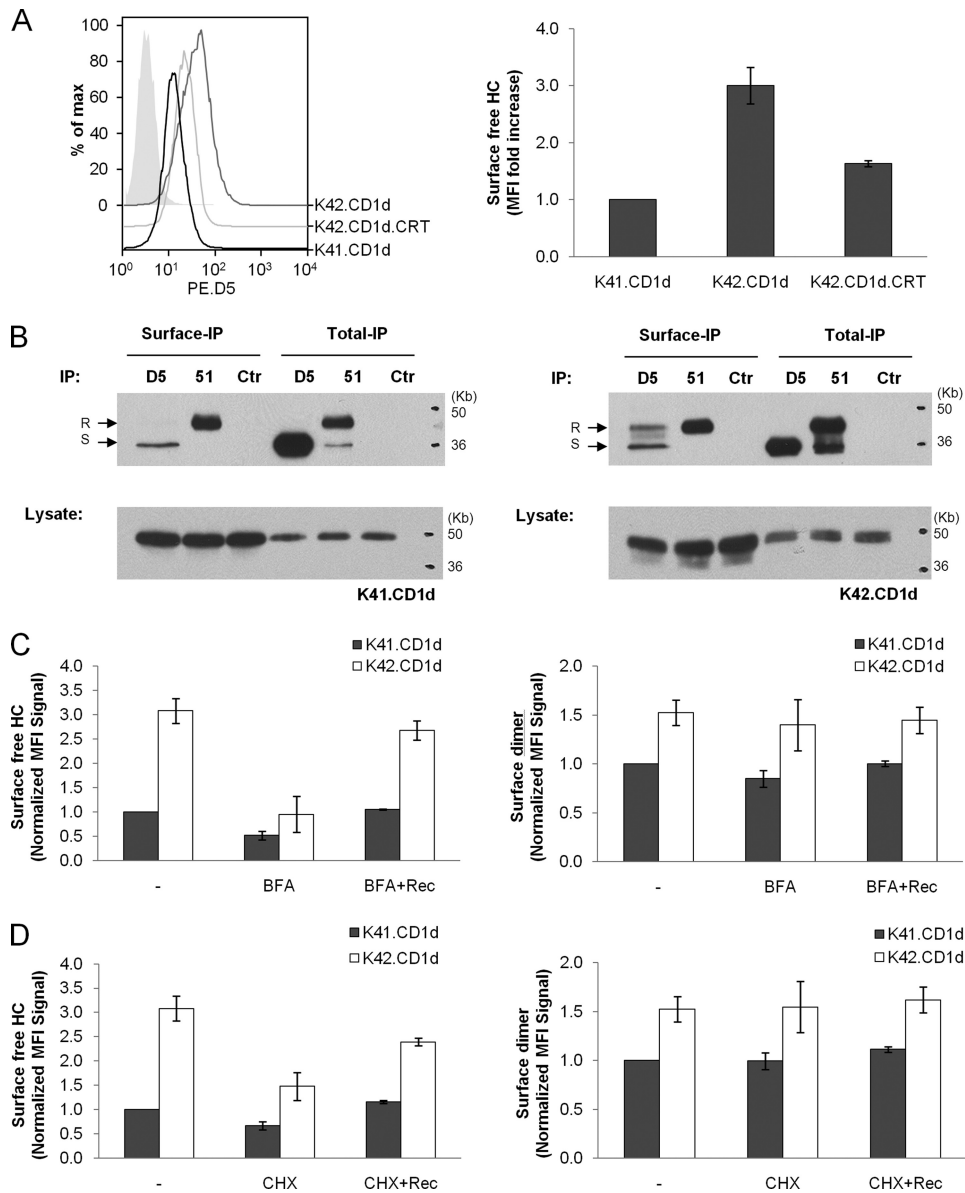


FIGURE 6. Escape of free CD1d heavy chains from the ER in the absence of CRT. *A*, the surface expression of CD1d heavy chains on K41.CD1d, K42.CD1d and K42.CD1d.CRT cells was examined by flow cytometry using the D5 antibody (unfilled histograms, *left panel*). Background staining was analyzed by incubating with secondary antibody alone (filled histogram, *left panel*). *Right panel*, statistical analysis of the data in the *left panel*. MFI values of K42.CD1d and K42.CD1d.CRT were normalized against that of K41.CD1d cells. Data shown are the average \pm S.E. of three separate experiments. *B*, the presence of free CD1d heavy chains on the surface of K42.CD1d cells examined by immunoprecipitation. The total CD1d in K41.CD1d and K42.CD1d cells was recovered by immunoprecipitation from a 1% digitonin cell lysate with D5 (anti-free heavy chain), CD1d51 (anti-CD1d/ β 2m dimer, 51) or a control antibody (Ctr) respectively (*Total-IP*). To capture the surface CD1d (*Surface-IP*), intact K41.CD1d or K42.CD1d cells were first incubated on ice for 30 min with D5, CD1d51 or a control antibody, washed, and extracted in 1% digitonin followed by the addition of protein G-Sepharose. Because the level of surface CD1d is much lower than that of the whole cell lysate, 10 times more cells were used for surface than total immunoprecipitations. Immunoprecipitates were SDS/DTT-eluted, digested with Endo H overnight, resolved by SDS-PAGE, and probed with biotin-labeled D5 antibody. The relative amounts of CD1d protein in each extract were assessed by directly immunoblotting the lysate. *C*, BFA treatment blocks the appearance of CD1d free heavy chains, but not dimers, on the cell surface. K41.CD1d and K42.CD1d cells were incubated at 37 °C for 4 h without (–) or with 10 μ g/ml BFA (*BFA*). *BFA-Rec*, cells were first incubated with BFA for 4 h, washed with PBS three times, and cultured at 37 °C to allow recovery. Cells were stained with D5 or CD1d51 antibodies to detect surface CD1d free heavy chains (*left panel*) or dimers (*right panel*), respectively. MFI values for each sample were normalized against untreated K41.CD1d cells (first black bar in *left and right panels* respectively). Data shown are the average \pm S.E. of three separate experiments. *D*, cycloheximide treatment also blocks the appearance of surface CD1d free heavy chains, but not dimers. The conditions were as in *C*, except cells were treated with 20 μ g/ml CHX instead of BFA.

molecules on the cell surface were properly assembled (Fig. 6*B*, *lane 2* in *left and right panels*). Additionally, and consistent with our flow cytometry results (Fig. 6*A*), a small amount of Endo

H-resistant free CD1d heavy chains was detected on the surface of K42.CD1d cells, but not of K41.CD1d cells (Fig. 6*B*, compare *lane 1* in *left and right panel*). The resistance to Endo H digestion suggests that they represent matured post-ER CD1d molecules. In contrast, the Endo H-sensitive D5-reactive CD1d detected both in K41.CD1d and K42.CD1d cells probably reflects an inevitable contamination by the vast excess of intracellular free CD1d heavy chains with immature glycans reported previously (26, 27, 51). The free CD1d heavy chains recovered from the total cell lysate are almost all Endo H-sensitive (Fig. 6*B*, *lane 4* in *left and right panels*), indicating that the vast majority is retained in the ER. Most of the β ₂m-associated dimers are Endo H-resistant, suggesting that they are post-ER populations, whereas only a fraction of dimers is Endo H-sensitive (Fig. 6*B*, *lane 5* in *left and right panels*). These probably represent recently assembled CD1d/ β ₂m complexes that have not yet reached the Golgi. We also observed that the ratio of CD1d51-reactive *versus* D5-reactive CD1d molecules was substantially higher for K42.CD1d than it was for K41.CD1d cells. This is consistent with the observed faster conversion rate of free CD1d heavy chains to dimers (Fig. 3, *A* and *B*) and the accumulation of Endo H resistant CD1d (Fig. 2*A*) in the absence of CRT. Taken together, the flow cytometry results and our biochemical data demonstrate the presence of free CD1d heavy chains on the surface of CRT-deficient cells.

Because CRT contains a KDEL ER retention sequence we speculated that the presence of D5-reactive CD1d on the surface of K42.CD1d cells is a result of the escape of free heavy chains normally retained by CRT. This hypothesis is also supported by the pulse-chase

data (Fig. 2, *B* and *C*), which indicated that CNX in K42.CD1d cells is not sufficient to retain CD1d molecules inside the ER. To examine this possibility, we treated K41.CD1d and K42.CD1d

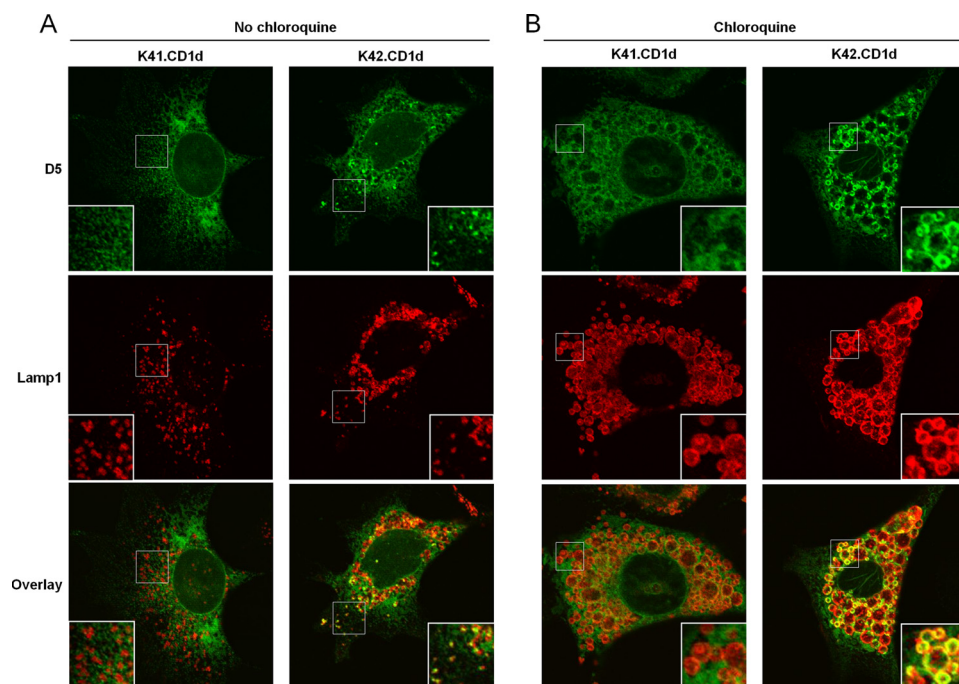


FIGURE 7. Rapid degradation of free surface CD1d heavy chains in CRT-deficient cells. *A*, subcellular localization of free CD1d heavy chains in lysosomes assessed by immunofluorescence. Fixed and permeabilized K41.CD1d and K42.CD1d cells were co-stained with D5 (anti-CD1d free heavy chains, green) and Lamp1 (red) antibodies. The overlay of two channels is on the bottom panels. Enlarged images of the selected areas are shown in the inserts. *B*, accumulation of CD1d free heavy chains in lysosomes after chloroquine treatment. Same as in *A*, except cells were treated with chloroquine overnight before staining to block lysosomal protein degradation.

cells with Brefeldin-A (BFA) and analyzed the effect on the expression of free surface CD1d heavy chains and dimers. BFA disrupts the structure and function of the Golgi apparatus and therefore blocks the transport of newly synthesized proteins to the cell surface. After 4 h of BFA treatment, the free heavy chains on the surface of K42.CD1d cells decreased significantly and this effect was almost fully reversible when the drug was removed and recovery of CD1d surface expression was allowed to occur (Fig. 6C, left panel). In contrast, the surface dimer levels were barely affected by BFA (Fig. 6C, right panel), which is consistent with the fact that the β_2m -associated CD1d dimer has a very long half-life and can continuously recycle between the surface and the endocytic pathway (15, 16, 22). These results suggest that the surface free CD1d heavy chains observed in K42.CD1d cells are derived from ER-escaped forms that have never been associated with β_2m rather than that they are continuously generated from recycling CD1d/ β_2m dimers. This is also supported by the comparable stability of dimers assembled in K41.CD1d and K42.CD1d cells (supplemental Fig. S1). Analogous results were also observed when cells were treated with the protein synthesis inhibitor cycloheximide (CHX) instead of BFA (Fig. 6D).

Free Surface CD1d Heavy Chains Are Rapidly Degraded in CRT-deficient Cells—The rapid disappearance of free CD1d heavy chains from the cell surface after the BFA or CHX treatment suggested that they are unstable, perhaps being internalized into the endocytic pathway for degradation. Consistent with this hypothesis, we detected by immunofluorescence low levels of D5-reactive free heavy chains in LAMP1-

positive lysosomes of CRT-deficient K42.CD1d cells (Fig. 7A, see inserts on left panels), although as expected, most D5-reactive CD1d was localized to the ER. Lysosomal localization of free heavy chains was observed in about 20% of K42.CD1d cells, suggesting that these forms are rapidly degraded. No co-localization of D5-reactive free CD1d heavy chains with LAMP1 was detected in K41.CD1d cells. Strikingly, after treating the cells with chloroquine to inhibit lysosomal degradation, free CD1d heavy chains dramatically accumulated in the lysosomes of K42.CD1d cells (Fig. 7B, see inserts on right panels) and the number of cells exhibiting co-localization of D5-reactive CD1d with LAMP1 also increased drastically to about 80%. In contrast, no lysosomal accumulation of free CD1d heavy chains was observed in K41.CD1d cells. These findings indicate that free CD1d heavy chains synthesized in the absence of CRT can escape from the ER and their *N*-linked glycans pro-

cessed in the Golgi prior to expression on the cell surface. However, they then undergo endocytosis and rapid lysosomal degradation.

DISCUSSION

Shortly after translocation into the ER, two of the three terminal glucose residues on the newly acquired *N*-linked glycans of glycoproteins are enzymatically trimmed to generate the monoglucosylated species that binds to CRT or CNX. This initiates the CRT/CNX/ERp57-dependent folding cycle in which the enzymes glucosidase II and UDP-glucose glycoprotein transferase work together to ensure correct conformation and disulfide bond formation. In the case of CD1d, disulfide bond formation is complete before association of the heavy chain with β_2m , and CRT or CNX do not interact with CD1d/ β_2m dimers (15). This suggests that folding of heavy chains is complete before β_2m association. CD1d has four *N*-linked glycans, and CD1d heavy chains form a ternary complex with both CRT and CNX that also associates with ERp57. Despite the simultaneous interaction of CD1d heavy chains with both lectins, CRT and CNX are not equivalent in their ability to mediate CD1d folding. While CNX deficiency has no discernable effect on the process (15),³ here we show accelerated assembly of CD1d heavy chains with β_2m , incomplete ER retention of free CD1d heavy chains, and increased accumulation of functional stable heterodimers in the absence of CRT. Therefore, CRT appears more critical than CNX in regulating CD1d folding and assembly.

³ P. Cresswell, unpublished data.

Because complete disulfide bond formation in CD1d heavy chains occurs before β_2m association, the accelerated assembly with β_2m in the absence of CRT also suggests that the oxidative folding of heavy chains is faster, and consistent with this we observed a considerably shorter association of CNX with heavy chains in CRT-deficient cells than in the wild-type cells (supplemental Fig. S2). Accelerated folding and assembly and shorter CNX interaction in CRT-depleted cells have also been reported for other glycoproteins, including influenza viral protein hemagglutinin, Semliki forest viral protein E1 and p62, and a few other cellular glycoproteins (52). Because the folding efficiency in these cases is slightly compromised in the absence of CRT, an extension of the folding cycle mediated by CRT may be required for optimal folding. However, we observed no difference in the stability of CD1d/ β_2m dimers assembled in CRT-deficient cells or wild-type cells, and the presentation of exogenous lipids was not impaired. This may be because other chaperones can substitute for CRT, as suggested by the enhanced interaction of CD1d heavy chains with Grp94 and Bip in the absence of CRT. However, other chaperones cannot completely replace the lectin chaperones; if cells are treated with CST during starvation, label, and chase to block the association with both CNX and CRT, disulfide bond formation in CD1d heavy chains is substantially impaired (15). In addition, when a CD1d mutant completely lacking *N*-linked glycans was stably expressed in human C1R cells, no assembly or surface expression of heavy chain- β_2m dimers was observed (25). Therefore, at least one of the lectin chaperones is likely to be required for correct CD1d heavy chain folding.

Although the assembly of CD1d/ β_2m dimers is accelerated in the absence of CRT, once formed the rate of egress from the ER of the dimers is identical (Fig. 2B). For MHC class I, transport is accelerated and the cohort of associated peptides on the cell surface is suboptimal, apparently because CRT-dependent recycling in the early secretory pathway is required for high affinity peptide loading (36). In the absence of CRT, sub-optimally loaded class I molecules escape the quality control system and cannot be retrieved to the ER for repeated rounds of peptide loading. Although CRT depletion does not affect loading and presentation of α -GalCer and GalGalCer to CD1d that is recycling in the endocytic system, the loading of self lipids to newly synthesized CD1d in the ER might be impaired as a result of inefficient ER retention. We have previously shown that the lipids bound by CD1d molecules appear to reflect the intracellular environments to which they have access (30). For example, soluble CD1d molecules restricted to the early secretory pathway by the addition of an ER retention signal at the C terminus are predominantly loaded with phosphatidylcholine, the most abundant phospholipid in the cell. Secreted soluble CD1d lacks easily detectable phosphatidylcholine but is associated with sphingomyelin, which it presumably acquires during transit through the secretory pathway. Hence the extended stay inside the ER mediated by CRT might modify the self lipid population associated with CD1d and potentially affect recognition by autoreactive NKT cells. However, CD1d molecules loaded with different self lipid populations may have similar stability and therefore be difficult to distinguish by traditional biochemical approaches.

Another direct effect of inefficient ER retention in CRT-deficient cells is the escape of free CD1d heavy chains from the ER and their subsequent expression on the plasma membrane. As mentioned previously, β_2m association is not strictly required for CD1d exit from the ER; the surface expression of free CD1d heavy chains has been reported in β_2m -deficient cells (27). In that case the glycans of the free CD1d heavy chains were immature, *i.e.* Endo H-sensitive, but appeared to retain function (28, 29). However, the free CD1d heavy chains on the surface of CRT-deficient cells carried Endo H-resistant, mature, *N*-linked glycans, and were rapidly lysosomally degraded, indicating that β_2m is required for the normal resistance of CD1d to lysosomal degradation.

As a result of faster assembly and inefficient ER retention, more stable and functional CD1d/ β_2m dimers accumulate on the cell surface in the absence of CRT. Re-expressing CRT in CRT-deficient cells partially reduces CD1d accumulation, and the level of CD1d expression and related NTK activation seem to correlate with the amount of CRT expressed. This suggests that CRT levels could potentially regulate CD1d-mediated stimulation of NKT cells. When, for example, CRT levels are up-regulated by initiation of the ER stress response (53), then CD1d levels may fall and NKT stimulation could be reduced. Similarly, cytokine-mediated induction of enhanced glycoprotein synthesis could generate competitors for CRT, enhancing CD1d expression. In preliminary experiments we have found that when wild-type MEFs expressing CD1d are treated with IFN- γ , which stimulates the expression of new glycoproteins such as MHC class I and class II molecules (54), the rate of assembly of CD1d/ β_2m increases, ER retention is reduced and more functional CD1d/ β_2m dimers are expressed on the cell surface (data not shown). This increase is not seen in CRT-negative MEFs, which is consistent with the hypothesis that CRT can regulate CD1d expression. However, further work is required to determine the underlying mechanisms and physiological significance of these observations.

Acknowledgments—We thank Drs. Crina Paduraru and Ralf M. Leonhardt for valuable discussions and Nancy Dometios for assistance with manuscript preparation.

REFERENCES

1. Brigl, M., and Brenner, M. B. (2004) *Annu. Rev. Immunol.* **22**, 817–890
2. Zeng, Z., Castaño, A. R., Segelke, B. W., Stura, E. A., Peterson, P. A., and Wilson, I. A. (1997) *Science* **277**, 339–345
3. Koch, M., Stronge, V. S., Shepherd, D., Gadola, S. D., Mathew, B., Ritter, G., Fersht, A. R., Besra, G. S., Schmidt, R. R., Jones, E. Y., and Cerundolo, V. (2005) *Nat. Immunol.* **6**, 819–826
4. Silk, J. D., Salio, M., Brown, J., Jones, E. Y., and Cerundolo, V. (2008) *Annu. Rev. Cell Dev. Biol.* **24**, 369–395
5. Beckman, E. M., Porcelli, S. A., Morita, C. T., Behar, S. M., Furlong, S. T., and Brenner, M. B. (1994) *Nature* **372**, 691–694
6. Barral, D. C., and Brenner, M. B. (2007) *Nat. Rev. Immunol.* **7**, 929–941
7. Bendelac, A., Lantz, O., Quimby, M. E., Yewdell, J. W., Bennink, J. R., and Brutkiewicz, R. R. (1995) *Science* **268**, 863–865
8. Wang, J., Li, Y., Kinjo, Y., Mac, T. T., Gibson, D., Painter, G. F., Kronenberg, M., and Zajonc, D. M. (2010) *Proc. Natl. Acad. Sci. U.S.A.* **107**, 1535–1540
9. Kinjo, Y., Wu, D., Kim, G., Xing, G. W., Poles, M. A., Ho, D. D., Tsuji, M., Kawahara, K., Wong, C. H., and Kronenberg, M. (2005) *Nature* **434**,

- 520–525
10. Mattner, J., Debord, K. L., Ismail, N., Goff, R. D., Cantu, C., 3rd, Zhou, D., Saint-Mezard, P., Wang, V., Gao, Y., Yin, N., Hoebe, K., Schneewind, O., Walker, D., Beutler, B., Teyton, L., Savage, P. B., and Bendelac, A. (2005) *Nature* **434**, 525–529
 11. Zhou, D., Mattner, J., Cantu, C., 3rd, Schrantz, N., Yin, N., Gao, Y., Sagiv, Y., Hudspeth, K., Wu, Y. P., Yamashita, T., Teneberg, S., Wang, D., Proia, R. L., Lavery, S. B., Savage, P. B., Teyton, L., and Bendelac, A. (2004) *Science* **306**, 1786–1789
 12. Kinjo, Y., Tupin, E., Wu, D., Fujio, M., Garcia-Navarro, R., Benhnia, M. R., Zajonc, D. M., Ben-Menachem, G., Ainge, G. D., Painter, G. F., Khurana, A., Hoebe, K., Behar, S. M., Beutler, B., Wilson, I. A., Tsuji, M., Sellati, T. J., Wong, C. H., and Kronenberg, M. (2006) *Nat. Immunol.* **7**, 978–986
 13. Bendelac, A., Savage, P. B., and Teyton, L. (2007) *Annu. Rev. Immunol.* **25**, 297–336
 14. Brutkiewicz, R. R., Bennink, J. R., Yewdell, J. W., and Bendelac, A. (1995) *J. Exp. Med.* **182**, 1913–1919
 15. Kang, S. J., and Cresswell, P. (2002) *J. Biol. Chem.* **277**, 44838–44844
 16. Jayawardena-Wolf, J., Benlagha, K., Chiu, Y. H., Mehr, R., and Bendelac, A. (2001) *Immunity* **15**, 897–908
 17. Elewaut, D., Lawton, A. P., Nagarajan, N. A., Maverakis, E., Khurana, A., Honing, S., Benedict, C. A., Sercarz, E., Bakke, O., Kronenberg, M., and Prigozy, T. I. (2003) *J. Exp. Med.* **198**, 1133–1146
 18. Gumperz, J. E. (2006) *Traffic* **7**, 2–13
 19. Zhou, D., Cantu, C., 3rd, Sagiv, Y., Schrantz, N., Kulkarni, A. B., Qi, X., Mahuran, D. J., Morales, C. R., Grabowski, G. A., Benlagha, K., Savage, P., Bendelac, A., and Teyton, L. (2004) *Science* **303**, 523–527
 20. Kang, S. J., and Cresswell, P. (2004) *Nat. Immunol.* **5**, 175–181
 21. Yuan, W., Qi, X., Tsang, P., Kang, S. J., Illarionov, P. A., Besra, G. S., Gumperz, J., and Cresswell, P. (2007) *Proc. Natl. Acad. Sci. U.S.A.* **104**, 5551–5556
 22. Chiu, Y. H., Park, S. H., Benlagha, K., Forestier, C., Jayawardena-Wolf, J., Savage, P. B., Teyton, L., and Bendelac, A. (2002) *Nat. Immunol.* **3**, 55–60
 23. Roberts, T. J., Sriram, V., Spence, P. M., Gui, M., Hayakawa, K., Bacik, I., Bennink, J. R., Yewdell, J. W., and Brutkiewicz, R. R. (2002) *J. Immunol.* **168**, 5409–5414
 24. Kang, S. J., and Cresswell, P. (2002) *EMBO J.* **21**, 1650–1660
 25. Paduraru, C., Spiridon, L., Yuan, W., Bricard, G., Valencia, X., Porcelli, S. A., Illarionov, P. A., Besra, G. S., Petrescu, S. M., Petrescu, A. J., and Cresswell, P. (2006) *J. Biol. Chem.* **281**, 40369–40378
 26. Balk, S. P., Burke, S., Polischuk, J. E., Frantz, M. E., Yang, L., Porcelli, S., Colgan, S. P., and Blumberg, R. S. (1994) *Science* **265**, 259–262
 27. Kim, H. S., Garcia, J., Exley, M., Johnson, K. W., Balk, S. P., and Blumberg, R. S. (1999) *J. Biol. Chem.* **274**, 9289–9295
 28. Brossay, L., Jullien, D., Cardell, S., Sydora, B. C., Burdin, N., Modlin, R. L., and Kronenberg, M. (1997) *J. Immunol.* **159**, 1216–1224
 29. Amano, M., Baumgarth, N., Dick, M. D., Brossay, L., Kronenberg, M., Herzenberg, L. A., and Strober, S. (1998) *J. Immunol.* **161**, 1710–1717
 30. Yuan, W., Kang, S. J., Evans, J. E., and Cresswell, P. (2009) *J. Immunol.* **182**, 4784–4791
 31. Joyce, S., Woods, A. S., Yewdell, J. W., Bennink, J. R., De Silva, A. D., Boesteanu, A., Balk, S. P., Cotter, R. J., and Brutkiewicz, R. R. (1998) *Science* **279**, 1541–1544
 32. Cox, D., Fox, L., Tian, R., Bardet, W., Skaley, M., Mojsilovic, D., Gumperz, J., and Hildebrand, W. (2009) *PLoS One* **4**, e5325
 33. Dougan, S. K., Salas, A., Rava, P., Agyemang, A., Kaser, A., Morrison, J., Khurana, A., Kronenberg, M., Johnson, C., Exley, M., Hussain, M. M., and Blumberg, R. S. (2005) *J. Exp. Med.* **202**, 529–539
 34. Zeissig, S., Dougan, S. K., Barral, D. C., Junker, Y., Chen, Z., Kaser, A., Ho, M., Mandel, H., McIntyre, A., Kennedy, S. M., Painter, G. F., Veerapen, N., Besra, G. S., Cerundolo, V., Yue, S., Beladi, S., Behar, S. M., Chen, X., Gumperz, J. E., Breckpot, K., Raper, A., Baer, A., Exley, M. A., Hegele, R. A., Cuchel, M., Rader, D. J., Davidson, N. O., and Blumberg, R. S. (2010) *J. Clin. Invest.* **120**, 2889–2899
 35. Gao, B., Adhikari, R., Howarth, M., Nakamura, K., Gold, M. C., Hill, A. B., Klee, R., Michalak, M., and Elliott, T. (2002) *Immunity* **16**, 99–109
 36. Howe, C., Garstka, M., Al-Balushi, M., Ghanem, E., Antoniou, A. N., Fritzsche, S., Jankevicius, G., Kontouli, N., Schneeweiss, C., Williams, A., Elliott, T., and Springer, S. (2009) *EMBO J.* **28**, 3730–3744
 37. Ireland, B. S., Brockmeier, U., Howe, C. M., Elliott, T., and Williams, D. B. (2008) *Mol. Biol. Cell* **19**, 2413–2423
 38. van den Elzen, P., Garg, S., León, L., Brigl, M., Leadbetter, E. A., Gumperz, J. E., Dascher, C. C., Cheng, T. Y., Sacks, F. M., Illarionov, P. A., Besra, G. S., Kent, S. C., Moody, D. B., and Brenner, M. B. (2005) *Nature* **437**, 906–910
 39. Spiro, R. G., Zhu, Q., Bhoyroo, V., and Söling, H. D. (1996) *J. Biol. Chem.* **271**, 11588–11594
 40. Ware, F. E., Vassilakos, A., Peterson, P. A., Jackson, M. R., Lehman, M. A., and Williams, D. B. (1995) *J. Biol. Chem.* **270**, 4697–4704
 41. Hebert, D. N., Foellmer, B., and Helenius, A. (1995) *Cell* **81**, 425–433
 42. Cannon, K. S., and Helenius, A. (1999) *J. Biol. Chem.* **274**, 7537–7544
 43. Liu, J., Shaji, D., Cho, S., Du, W., Gervay-Hague, J., and Brutkiewicz, R. R. (2010) *J. Immunol.* **184**, 4973–4981
 44. Yu, K. O., Im, J. S., Molano, A., Dutronc, Y., Illarionov, P. A., Forestier, C., Fujiwara, N., Arias, I., Miyake, S., Yamamura, T., Chang, Y. T., Besra, G. S., and Porcelli, S. A. (2005) *Proc. Natl. Acad. Sci. U.S.A.* **102**, 3383–3388
 45. Kawano, T., Cui, J., Koezuka, Y., Taura, I., Kaneko, Y., Motoki, K., Ueno, H., Nakagawa, R., Sato, H., Kondo, E., Koseki, H., and Taniguchi, M. (1997) *Science* **278**, 1626–1629
 46. Brossay, L., Chioda, M., Burdin, N., Koezuka, Y., Casorati, G., Dellabona, P., and Kronenberg, M. (1998) *J. Exp. Med.* **188**, 1521–1528
 47. Burdin, N., Brossay, L., Koezuka, Y., Smiley, S. T., Grusby, M. J., Gui, M., Taniguchi, M., Hayakawa, K., and Kronenberg, M. (1998) *J. Immunol.* **161**, 3271–3281
 48. Prigozy, T. I., Naidenko, O., Qasba, P., Elewaut, D., Brossay, L., Khurana, A., Natori, T., Koezuka, Y., Kulkarni, A., and Kronenberg, M. (2001) *Science* **291**, 664–667
 49. Leonhardt, R. M., Keusekotten, K., Bekpen, C., and Knittler, M. R. (2005) *J. Immunol.* **175**, 5104–5114
 50. Chefalo, P. J., Grandea, A. G., 3rd, Van Kaer, L., and Harding, C. V. (2003) *J. Immunol.* **170**, 5825–5833
 51. Somnay-Wadgaonkar, K., Nusrat, A., Kim, H. S., Canchis, W. P., Balk, S. P., Colgan, S. P., and Blumberg, R. S. (1999) *Int. Immunol.* **11**, 383–392
 52. Molinari, M., Eriksson, K. K., Calanca, V., Galli, C., Cresswell, P., Michalak, M., and Helenius, A. (2004) *Mol. Cell* **13**, 125–135
 53. Mintz, M., Vanderver, A., Brown, K. J., Lin, J., Wang, Z., Kaneski, C., Schiffmann, R., Nagaraju, K., Hoffman, E. P., and Hathout, Y. (2008) *J. Proteome Res.* **7**, 2435–2444
 54. Saha, B., Jyothi Prasanna, S., Chandrasekar, B., and Nandi, D. (2010) *Cytokine* **50**, 1–14